30 March 2001

ELSEVIER

Chemical Physics Letters 337 (2001) 117–124

CHEMICAL PHYSICS LETTERS

www.elsevier.nl/locate/cplett

Carrier recombination in clusters of NiO

Victor V. Volkov [a,*], Z.L. Wang [b], B.S. Zou [a]

[a] School of Chemistry and Biochemistry, Georgia Institute of Technology, Atlanta, GA 30332-0400, USA
[b] School of Materials Science and Engineering, Georgia Institute of Technology, Atlanta, GA 30332-0400, USA

Received 20 March 2000; in final form 5 February 2001

Abstract

We studied the dependence of carrier recombination pathways in nanoparticles of NiO on surface conditions. Two types of 0.6 nm short-range order clusters of NiO were prepared in reverse micelles of dodecyl benzene sulfonate. The steady-state absorption and time-resolved fluorescence measurements were done in order to investigate the photophysical properties of d–d in-gap transitions. The NiO nanoclusters and bulk steady-state optical absorption and emission properties are comparatively discussed from the prospective of Laporte's rules relaxation. The results of the time-resolved emission studies allowed us to develop the phenomenological model of the in-gap carrier recombination in NiO clusters.

1. Introduction

Quantum confinement gives powerful degrees of freedom in the modification of optical, magnetic and electronic properties of matter. The II–VI semiconductor particles are the most commonly studied materials during the last decade. Their structural and optical properties are well described. Carrier recombination in semiconductor particles is determined by the band gap character and by the presence of defects. In contrast, the optical properties and carrier-related phenomena in transition metal compounds are governed by d–d transitions present within the band gap.

Nickel oxide is a typical binary transition metal oxide with rock salt structure and antiferromagnetic properties below 523 K. The Ni^{2+} ion has the configuration $3s^23p^63d^8$. This transition metal ion has six O^{2-} surrounding ions to form an elementary octahedron with O_h symmetry. The oxygen ions' crystal field splits d-electron states into e_g and t_{2g} states. Their degeneracy is further lifted by exchange interactions, spin–orbital coupling and field distortions. NiO band structure and electronic properties were subjects of numerous theoretical and experimental studies [1–6]. The band gap for bulk nickel oxide was found to be about 4 eV, which is much smaller than the Mott–Hubbard correlation energy, U ($U \approx 7$–10 eV) [7,8]. Modern consideration classifies NiO as a charge-transfer insulator [9–16]. In reality, the existing density of d states within the band gap (even they do not form a continuum band) separates NiO into a special group of materials – very weak conductors.

All d–d transitions are dipole-forbidden by a parity selection rule. However, weak optical density [17], photoluminescence, and cathodoluminescence in the IR–VIS region [18] indicate a

* Corresponding author. Fax: +1-404-894-7452.
E-mail addresses: victor@chemistry.gatech.edu, victorvolkov@linuxmail.org (V.V. Volkov).

0009-2614/01/$ - see front matter
PII: S0009-2614(01)00191-9

relaxation of the parity rule due to lattice vibration couplings, quadrupole interactions, and band mixing (particularly near the conduction band) [19]. The understanding of NiO intra-atomic d–d transition properties is complicated by both the non-stoichiometry and the contribution of surface states. Quantum confinement allows the surface to play a more prominent and sometimes even a dominant role in the definition of structural, electronic and optical properties of matter. For example, the recent results of X-ray photoemission spectroscopy studies on capped NiO particles verify that thermal treatment causes higher covalency and Ni(d)–O(p) hybridization [20]. In this work we investigate optical absorption and emission of the short-range order NiO in the confined state. Our results allow us to consider surface states' contribution in carrier recombination pathways.

2. Experimental

1 nm size clusters of NiO coated with a layer of anionic surfactant molecules were prepared with the microemulsion method described in [20]. We developed two structurally related systems. NiO(1) is a result of refluxing at 110°C the as-prepared (in toluene) nanoclusters for 1 h. NiO(2) particles underwent at least 3 h refluxing at 250°C. The NiO(2) solvent has to be exchanged into xylenes in order to perform the higher temperature refluxing.

The nanoclusters were studied by transmission electron microscopy (TEM), carried out at 200 kV using a Hitachi HF-2000. A droplet of the solution containing the clusters was dispersed on an ultrathin holey amorphous carbon film supported by a copper grid. The small size and the amorphous structure of the nanoclusters greatly reduced their visibility in conventional bright-field imaging. To image the clusters, we used the method of mass-thickness contrast in TEM, which was performed in dark-field mode by carefully positioning the objective aperture so that the scattering from the nanoclusters was enhanced, while that from the substrate was suppressed. Since the scattering power of an atom strongly depends on its atomic number, heavy atoms produce a strong higher angle scattering signal [21]. If the objective aperture picked up only a portion of the high angle scattering signal, the image would show the nanoclusters because of their higher atomic number. This is the so-called *Z*-contrast in TEM.

A Beckman DU-650 spectrophotometer was used to measure UV–VIS absorption spectra. The photoluminescence spectra of the NiO nanoclusters in reverse micelles were recorded using the QM-1 fluorescence system from Photon Technology International. A Bruker IFS66/S infrared spectrometer was used for infrared absorption studies.

Low temperature steady state and time-resolved fluorescence measurements on the nanoclusters were performed with the closed-cycle refrigerator system, Janis CCS-150, designed to operate between 10 and 325 K. We allowed at least 40 min settlement time for temperature stabilization before any data collection at each temperature.

The temporal behavior of nanoclusters' emission was measured using the time-correlated photon counting technique. The excitation source was 580 nm from a dye laser (Spectra-Physics, model 375B) with a cavity dumper. The dye laser was synchronously pumped by a mode-locked Nd:YAG laser (Spectra-a, model 3800). The pulse width was measured using an autocorrelator and found to be 35 ps. The detection system was a microchannel plate photomultiplier tube (Hamamatsu R1564) coupled with a pulse-to-height converter (ORTEC, model 457), which provided an instrument response function of 60 ps (FWHM). The fluorescence decay was collected until 10 000 counts were obtained.

3. Results and discussion

A dark-field image recorded using the method introduced above is given in Fig. 1. The electron diffraction (Fig. 1, top right corner insert) demonstrates that NiO(1) clusters possess short-range order. The NiO(2) clusters were found to be amorphous. The clusters exhibit bright contrast. The size statistics suggest a distribution for the clusters' diameter around 0.6 nm with 0.5 nm FWHM. This measurement could underestimate

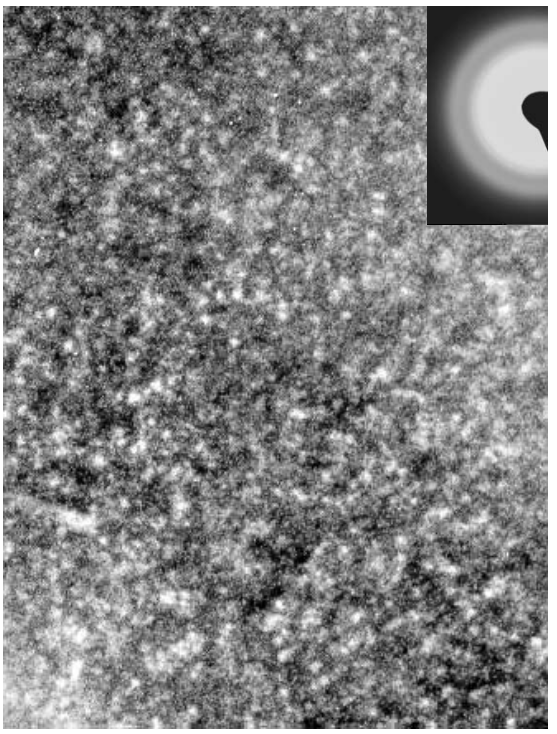

Fig. 1. Dark-field TEM image of NiO clusters with short-range order.

the size of the clusters because the image is sensitive only to the thicker clusters regions. Therefore the clusters could be 20–30% larger.

The inductively coupled plasma atomic emission spectroscopy allowed us to estimate the concentrations of Ni^{2+} in NiO(1) and NiO(2) systems to be 4.3 and 0.15 g/l, respectively. We compared the presence of intra-micelle water in the two systems using the characteristic 3200–3500 cm^{-1} OH stretch in the IR spectrum. According to IR absorption spectra, NiO(1) micelles contain interfacial water, while the NiO(2) surface is dry, therefore DBS molecules are in close contact with it. The surfactant band at 1011 cm^{-1} indicates a 5-fold decrease of the DBS concentration in NiO(2) during refluxing compared to NiO(1). This result is consistent with dry sample weight analysis. Quantitative chemical microanalysis by energy dispersive X-ray spectroscopy quantified Ni, O, and S atoms on the grids to be 22, 49, 44 for NiO(1) and 22, 56, 22 for NiO(2), respectively. The level of oxygen is very low in both systems what suggests that nickel ions and surfactant molecules probably share oxygen on the surface. The higher level of oxygen in NiO(2) clusters suggests a slight oxygen doping.

The absorption spectra of NiO nanoclusters are given in Fig. 2. The shown spectra are corrected for the concentration of Ni^{2+} and the solvent contribution. Both samples demonstrate a similar series of d–d transitions to those observed in NiO bulk [17,22,23]. NiO bulk demonstrates three bands of optical transitions below the charge transfer transition (~4 eV). The assignment of the Ni^{2+} d band transitions is still ambiguous. The observed in-gap optical density has often been the subject of numerous theoretical investigations [24–28].

The observed optical absorption features of Ni^{2+} ions are considered in terms of the ligand field theory. In octahedral coordination, Ni^{2+}

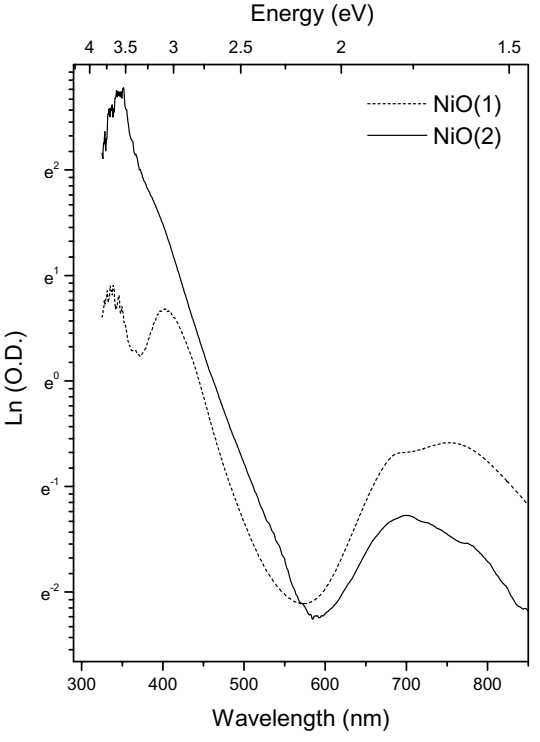

Fig. 2. Absorption spectra of NiO(1) (dashed line) and NiO(2) (solid line) nanoclusters.

demonstrates three absorption bands due to the transitions from the ground state $^3A_{2g}$ to the $^3T_{2g}$, $^3T_{1g}(F)$ and $^3T_{1g}(G)$ states. These transitions are at 1, 1.7 and 3.2 eV, respectively, and show a complex substructure due to spin–orbital interaction and local distortions [17,22].

The electric dipole d–d transitions are restricted according to Laporte's rule. Recently, Rossman et al. [22] reported the theoretical calculations (within Hartree–Fock formalism) of the magnetic dipole and electric quadrupole contributions to the absorption cross-section. They demonstrated a very reasonable fit of the optical absorption spectra. However, the amplitudes of the calculated features are 1–2 orders smaller than observed experimentally. Additionally, they showed that the O(p)–Ni(d) electron hybridization contribution into the relaxation of the parity rules is negligible for the in-gap states. Hence, it was suggested that the optical absorption spectra of Ni^{2+} ions arise due to the participation of the odd vibrational modes.

The NiO clusters' optical transitions are broad, even at 10 K. The spectral broadening arises as a result of local structural variance. We observed no Ni^{2+} optical absorption in the 0.6–1 eV spectral range in neither system. According to the calculations by Rossman et al. [22] the broad band of NiO bulk in the spectral range of 0.6–1 eV is purely magnetic dipole in nature. Prepared clusters of NiO are amorphous to a large extent, therefore the magnetic order is lost within the matter. Thus, this observation lends support to their calculations.

The clusters of NiO(2) demonstrate a slight reduction of the amplitudes of the optical transitions to the $^3T_{2g}(F)$ state compared to NiO(1). On the other hand, the high temperature treated sample shows a low energy charge transfer band-tail, therefore its color is no longer green, as in the case of NiO(1), but yellow. The optical transitions to the $^3T_{2g}(F)$ state may be completely covered as a result of such modification, see [20]. Both the charge transfer low energy band-tail and the increase of its amplitude was correlated by Rossman et al. [22] with the distortion of the octahedral symmetry of the Ni^{2+} site and/or Ni valency change. This is in agreement with the stronger disorder of the NiO(2) clusters. The higher temperature treatment results in a stronger Madelung potential of the surfactant on the surface. Surface induced lattice reorganization leading to amorphization was observed in a variety of small binary oxides particles [29].

Finally, the optical absorption of NiO does not show a blue shift upon size reduction. Hence, there is no confinement of the carriers involved in the d–d transitions due to their very small Bohr radii. Such is probably not the case when the carriers are excited with higher energy. The X-ray photoemission studies on clusters of NiO revealed a higher energy shift of the valence band emission compared to NiO bulk. This was considered to be a result of confinement of the hole formed in the Ni 2p state [20].

Fig. 3a represents room temperature steady-state emission from clusters of NiO(1) and neat solvent. When pumped above 3 eV, the observed photoluminescence contains structured contribution from the toluene. The solvent component becomes negligible when the excitation wavelength is lower than 2.95 eV (absorption edge). The photoluminescence of the 3 year old clusters of NiO(1) is similar to that of freshly prepared sample but lacks the solvent component. The given spectra of NiO(1) clusters demonstrate broad photoluminescence with a maximum around 2.25 eV. The photoluminescence properties of the NiO(1) and NiO(2) clusters are shown comparatively in Fig. 3b. The emission from NiO(2) is red shifted and is 2 orders of magnitude stronger than the photoemission from NiO(1).

It was reported recently that radiative recombination of carriers in NiO bulk consists of two photoemission maxima, one at 3.2 eV and a larger one at 2.8 eV [18]. When compared to the bulk, the photoluminescence from the clusters of NiO is broad, red shifted and slightly dependent with its maximum on the excitation wavelength. These features are due to carrier thermalization on tail states formed as a result of the amorphous nature of the clusters. The spectral character of the reported data implies that the $^1T_{2g}(D)$, $^3T_{1g}(P)$ and possibly ^1E_g states contribute to the carrier radia-

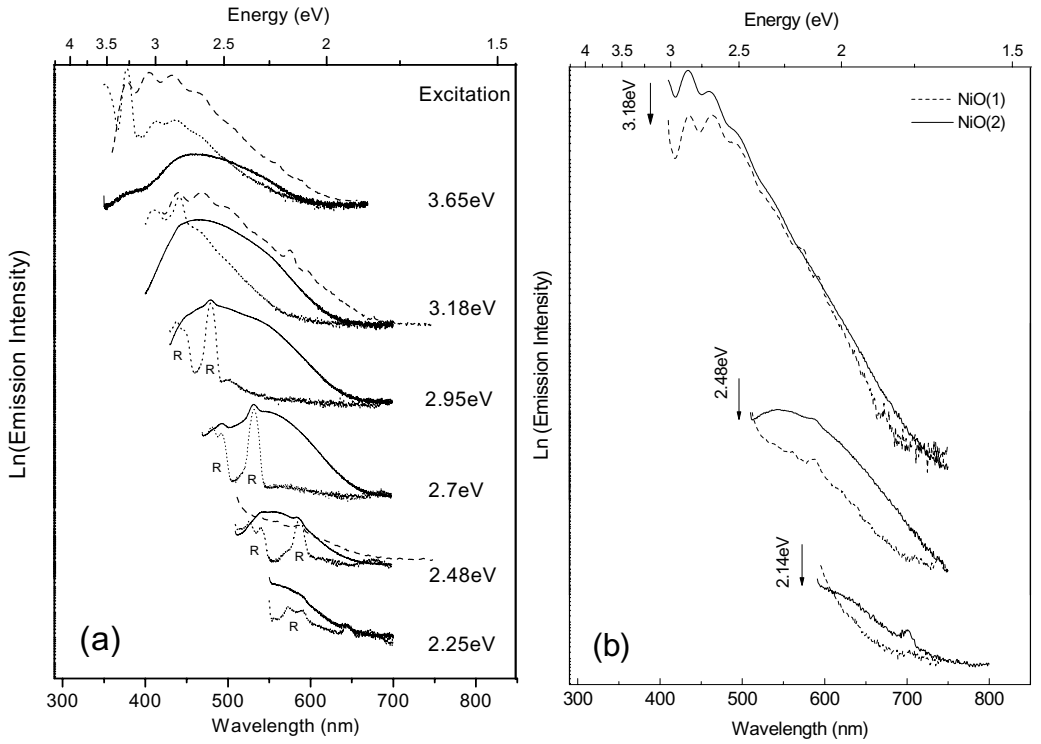

Fig. 3. Near UV–VIS steady-state emission spectra of clusters of: (a) NiO(1) as prepared (dashed line) and 3 years old (solid line) under given excitations and (b) NiO(1) (dashed line) and NiO(2) (solid line) clusters upon 3.18, 2.48 and 2.14 eV excitations. Neat toluene spectra are shown with dotted line. Letter 'R' marks the Raman contribution.

tive recombination. However, the higher quantum yield in NiO(2) clusters suggests the special role of the surface induced local non-cubic distortions in photoemission enhancement.

Fig. 4 represent time-resolved photoluminescence decays from NiO nanoclusters at different temperatures. The excitation at 584 nm (2.12 eV) promotes in-gap $^1T_{2g}$ and ^1E_g d–d transitions only. Hence, the detected emission comes from comparatively lower in-gap d states. We fitted the emission decay with two lifetime components in the range of 30–70 ps, 300–500 ps. Both estimated lifetimes are shorter for NiO(1) than for NiO(2). The first component is a dominant one in NiO(1) and noticeable in NiO(2) at room temperature. As may be seen in Fig. 4b, we were able to freeze out the first component and observe the carrier recombination in NiO(2) with $\tau \approx 500$ ps. At low temperature we anticipate the appearance of a small third lifetime component (2–3 ns) in NiO(2) only. Our results suggest that the first lifetime component (30–70 ps) can be assigned to the purely nonradiative recombination center. The Arrhenius plots for the fast component (insets in Fig. 4) give an estimate of the activation energies in NiO(1) and NiO(2) of 7 and 10 meV, respectively.

It was shown that NiO bulk has two emitting states with lifetimes of 10 μs and 75–200 ms [18]. Our observation indicates that the NiO size reduction and amorphization do not alter the pathways of relaxation. However, there are two important trends in clusters of NiO we have to take into account: the decrease of the recombination lifetimes in clusters compared to the bulk, and the modification of carrier recombination pathways upon temperature treatment of the prepared clusters.

The decrease of the lifetime upon size reduction was observed and discussed recently for Mn^{2+}

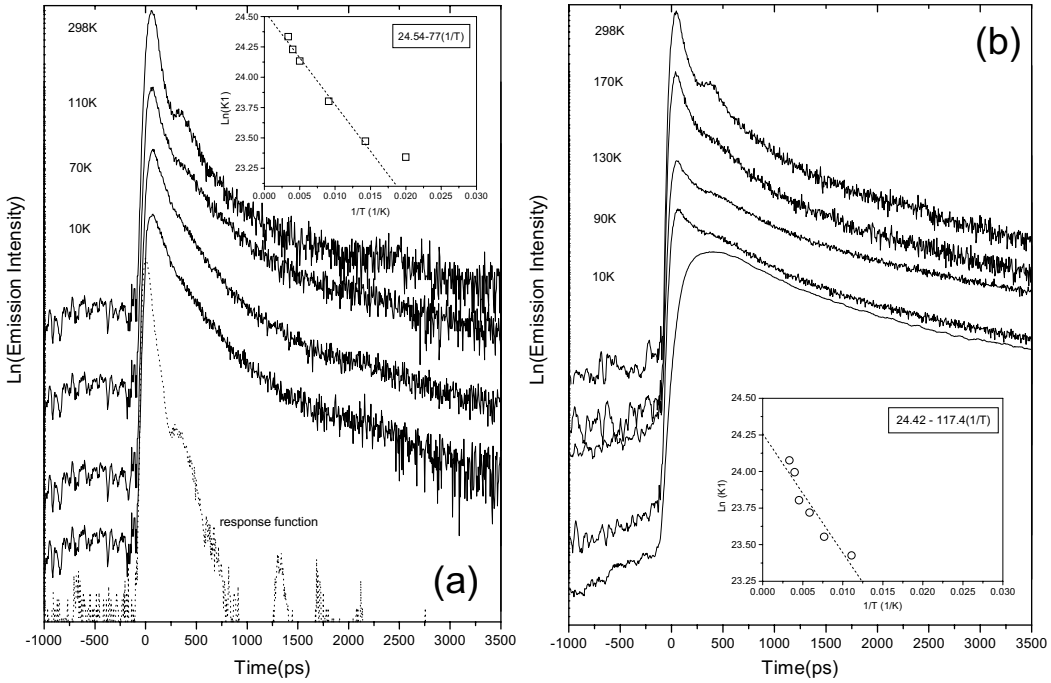

Fig. 4. Time-resolved emission from clusters of: (a) NiO(1) at 298, 110, 70 and 10 K and (b) NiO(2) at 298, 170, 130, 90 and 10 K. Response function is given by dotted line. Insets give the Arrhenius plots for the emission fast component, respectively.

doped ZnS nanocrystals [30]. The faster recombination was explained as a result of the carrier Bohr radius reduction and the formation of the d-orbital bound state in the nanocrystals. This consideration seems to be plausible since we can expect the presence of very localized sates in amorphous clusters of NiO. However, this is valid for the system where nonradiative recombination contribution is small. Around 550 nm the quantum yield of the emission from NiO(1) and NiO(2) is estimated to be 10^{-5} and 10^{-3} at 298 K (10^{-4} and 0.03 at 10 K), respectively. Therefore, we consider the faster recombination in clusters to be a result of the nonradiative recombination pathway enhancement.

Fig. 5 represents the carrier recombination scheme we have developed to explain the NiO clusters optical emission properties. First of all, we consider the presence of the two recombination sites according to the number of lifetime and spectral components in clusters and in bulk of NiO. The first site channels the fast and nonradiative recombination predominantly. It is populated via phonon assisted hopping overa barrier, which is formed as a result of the potential curve displacement. We consider that in NiO(2) both the

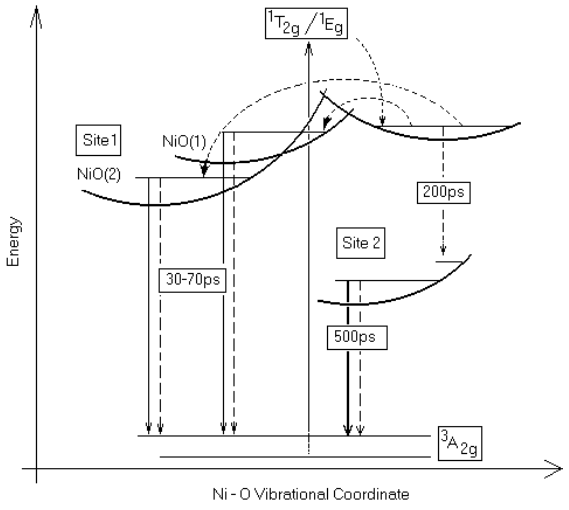

Fig. 5. General scheme of the carrier recombination pathways in clusters of NiO. The nonradiative and radiative transitions are depicted with dashed and solid arrows, respectively.

longer recombination from site1 and the decrease of its fraction upon cooling are due to the relatively higher activation energy (see Arrhenius plots in Fig. 4). The larger displacement of the NiO(2) site1 potential curve is in agreement with the stronger electron–phonon coupling reported by Zou et al. [20]. The second site successfully competes with the first one at low temperature only. It is populated nonradiatively within 200 ps. The carrier recombination from the site2 demonstrates an increase of the radiative component.

The assignment of the discussed sites is ambiguous due to the lack of spectral resolution. Besides possible emission from the ^1E_g and $^3T_{2g}(F)$, states it is reasonable to expect the contribution from the tail of the $^1T_{2g}(D)$ state. The material analysis results and the character of the steady state and time-resolved emission indicate the importance of the local distortion of the octahedral symmetry of the Ni^{2+} ion for optical response. It was shown recently that the electron–phonon coupling constant and its sign can be estimated for particular state symmetry and it's local distortion [31]. Therefore, it is possible to think about the control of the distortion of the states in order to enhance the d–d transitions which show the high yield due to the effective mixing with the odd vibrational modes.

In conclusion, we investigated the steady-state and time-resolved optical properties of d–d transitions in NiO particles with short-range order. 1 nm clusters of NiO show strong optical absorption and emission properties dependent on the preparation conditions. The results of the time-resolved emission studies in NiO clusters allowed us to develop the phenomenological model of the in-gap carrier relaxation on d-states. Surfactant molecules coordination on the NiO surface gives rise to the non-cubic sites and facilitates the carrier radiative recombination pathway.

Acknowledgements

We thank Prof. M.A. El-Sayed for supplying the facility in carrying out the reported research and his encouragement. V.V.V., B.S.Z. and Z.L.W. thank respectively the Office of Naval Research (Grant No. DE-FG03-88ER-13828), the Molecular Design Institute at Georgia Institute of Technology and NSF (DMR-9733160), for financial support. V.V.V. thanks Dr. Z. Dai, Dr. J. Wang, J.S. Rainey III for help in clusters characterization, and C. Heyes for technical assistance.

References

[1] N.F. Mott, R. Peirls, Proc. Phys. Soc. (Extra Part) 49 (1937) 72.
[2] H.J. DeBoer, E.J.W. Verwey, Proc. Phys. Soc. (Extra Part) 49 (1937) 59.
[3] N.F. Mott, Proc. Phys. Soc. A 62 (1949) 416.
[4] J. Hubbard, Proc. R. Soc. London Ser. A 276 (1964) 238.
[5] J. Hubbard, Proc. R. Soc. London Ser. A 277 (1964) 237.
[6] J. Hubbard, Proc. R. Soc. London Ser. A 281 (1964) 401.
[7] R.J. Powell, W.E. Spicer, Phys. Rev. B 2 (1970) 2185.
[8] S. Hufner, P. Steiner, I. Sander, M. Neumann, S. Witzel, Z. Phys. B: Condens. Matter B 83 (1991) 185.
[9] N.F. Mott, The Metal Insulator Transition, Taylor & Francis, London, 1974.
[10] S. Hufner, F. Hulliger, J. Osterwalder, T. Riesterer, Solid State Commun. 50 (1984) 83.
[11] S. Hufner, Solid State Commun. 47 (1983) 493.
[12] S. Hufner, Z. Phys. B: Condens. Matter B 58 (1984) 1.
[13] S. Hufner, Z. Phys. B: Condens. Matter B 61 (1985) 135.
[14] A. Fujimori, F. Minami, S. Sugano, Phys. Rev. B 29 (1984) 5225.
[15] A. Fujimori, F. Minami, Phys. Rev. B 30 (1984) 957.
[16] G.A. Sawatzky, J.W. Allen, Phys. Rev. Lett. 53 (1984) 2339.
[17] T. Tsuboi, W. Kleemann, J. Phys.: Condens. Matter 41 (1994) 8625.
[18] C. Diaz-Guerra, A. Remon, J. Garcia, J. Piqueras, Phys. Stat. Sol. (a) 163 (1997) 497.
[19] S. Sugano, Y. Tanabe, H. Kamimura, Multiplets of Transition Metal Ions in Crystals, Academic Press, New York, 1970.
[20] B. Zou, L. Wang, J. Lin, Solid State Commun. 94 (1995) 847.
[21] Z.L. Wang, Elastic and Inelastic Scattering in Electron Diffraction and Imaging, Plenum Press, New York, 1995 (Chapters 1 and 6).
[22] G. Rossman, R. Shannon, R. Waring, J. Solid State Chem. 39 (1981) 277.
[23] C. Jorgensen, M. Lenglet, J. Arsene, Chem. Phys. Lett. 136 (1987) 475.
[24] A. Fujimori, F. Minami, Phys. Rev. B 30 (1984) 957.
[25] J. Hugel, M. Kamal, J. Phys.: Condens. Matter 9 (1997) 647.
[26] V. Anisimov, F. Aryasetiawan, A. Lichtenstein, J. Phys.: Condens. Matter 9 (1997) 767.

[27] S. Rossano, Ch. Brouder, M. Alouani, M.-A. Arrio, Phys. Chem. Minerals 27 (2000) 170.
[28] A. Freitag, V. Staemmler, D. Cappus, C. Ventrice, K. Al Shamery, H. Kuhlenbeck, H. Freund, Chem. Phys. Lett. 210 (1993) 10.
[29] B. Zou, V. Volkov, Z. Wang, Chem. Mater. 11 (1999) 3037.
[30] F. Jain, W. Huang, J. Appl. Phys. 85 (1999) 2706.
[31] K. Wissing, J. Degen, Mol. Phys. 95 (1998) 51.